JACS
JOURNAL OF THE AMERICAN CHEMICAL SOCIETY
Article
pubs.acs.org/JACS

Transfer Channel of Photoinduced Holes on a TiO_2 Surface As Revealed by Solid-State Nuclear Magnetic Resonance and Electron Spin Resonance Spectroscopy

Fen Liu,[†,‡] Ningdong Feng,*[,†] Qiang Wang,[†] Jun Xu,[†] Guodong Qi,[†] Chao Wang,[†] and Feng Deng*[,†]

[†]State Key Laboratory of Magnetic Resonance and Atomic and Molecular Physics, National Center for Magnetic Resonance in Wuhan, CAS Key Laboratory of Magnetic Resonance in Biological Systems, Wuhan Institute of Physics and Mathematics, Chinese Academy of Sciences, Wuhan 430071, People's Republic of China

[‡]University of Chinese Academy of Sciences, Beijing 100049, People's Republic of China

Supporting Information

ABSTRACT: The detailed structure−activity relationship of surface hydroxyl groups (Ti−OH) and adsorbed water (H_2O) on the TiO_2 surface should be the key to clarifying the photogenerated hole (h^+) transfer mechanism for photocatalytic water splitting, which however is still not well understood. Herein, one- and two-dimensional ^1H solid-state NMR techniques were employed to identify surface hydroxyl groups and adsorbed water molecules as well as their spatial proximity/interaction in TiO_2 photocatalysts. It was found that although the two different types of Ti−OH (bridging hydroxyl (OH_B) and terminal hydroxyl (OH_T) groups were present on the TiO_2 surface, only the former is in close spatial proximity to adsorbed H_2O, forming hydrated OH_B. In situ ^1H and ^{13}C NMR studies of the photocatalytic reaction on TiO_2 with different Ti−OH groups and different H_2O loadings illustrated that the enhanced activity was closely correlated to the amount of hydrated OH_B groups. To gain insight into the role of hydrated OH_B groups in the h^+ transfer process, in situ ESR experiments were performed on TiO_2 with variable H_2O loading, which revealed that the hydrated OH_B groups offer a channel for the transfer of photogenerated holes in the photocatalytic reaction, and the adsorbed H_2O could have a synergistic effect with the neighboring OH_B group to facilitate the formation and evolution of active paramagnetic intermediates. On the basis of experimental observations, the detailed photocatalytic mechanism of water splitting on the surface of TiO_2 was proposed.

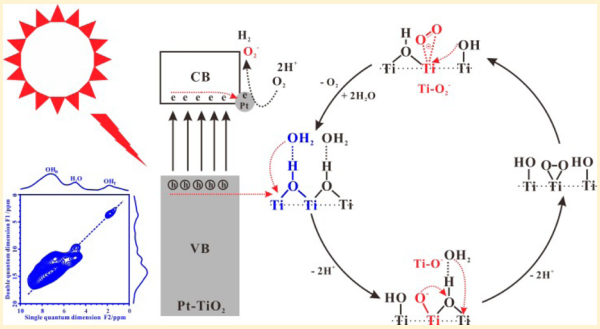

1. INTRODUCTION

As the crucial step of photoreaction on TiO_2 photocatalysts, the surface transfer of photoinduced holes (h^+) (that is, how the photoinduced holes transfer from the TiO_2 surface to adsorbed water and organic compounds on the surface active sites) has been received intensive attention[1−3] in terms of photocatalytic water (H_2O) splitting and photocatalytic environmental cleaning. However, the ambiguous knowledge of surface active sites hinders the identification of the h^+ transfer mechanism. Owing to the lack of direct experimental evidence, the most controversial point concerning the nature of surface active sites is whether the surface hydroxyl groups (Ti−OH) of TiO_2 can trap the photogenerated hole. Surface hydroxyl groups (Ti−OH) and adsorbed H_2O influence directly the physical and chemical properties of TiO_2 and thus may play important roles in photocatalytic reactions.[4−6] It has long been assumed that the Ti−OH groups and/or adsorbed H_2O may be the surface active species, which can be oxidized by photogenerated holes (h^+) to form a surface radical ($^-$O−Ti and/or $^\bullet$OH) with high oxidation activity.[4,7,8] In contrast, other research work[2,3,9,10] speculated that it was surface lattice oxygen (bridging oxygen, Ti−O−Ti) rather than the Ti−OH groups with adsorbed H_2O that acted as the surface active species, which could trap the photogenerated h^+ and be oxidized to form Ti−O^- radicals as the energy level of Ti−OH groups and adsorbed H_2O were both far below the top of the valence band of TiO_2. However, theoretical results[11,12] indicated that such an energy mismatch between the valence band and the electronic states of Ti−OH groups and adsorbed H_2O could be overcome by the overpotential created by the photogenerated hole in the vicinity of Ti−OH groups and adsorbed H_2O, resulting in their photooxidation. Therefore, the detailed insight into the structure−activity relationship of surface Ti−OH groups and adsorbed H_2O should be the key to clarifying the photocatalytic mechanism on the TiO_2 surface. It has been found so far that two types of Ti−OH groups (terminal and bridging hydroxyl groups) were present on the surface of TiO_2,[6,13−16] whereas their distinct distribution and activity properties still remained unclear. Furthermore, the detailed role of adsorbed H_2O in the

Received: May 11, 2017
Published: July 7, 2017

DOI: 10.1021/jacs.7b04877
J. Am. Chem. Soc. 2017, 139, 10020−10028

formation of surface active sites and the h^+ transfer process has been scarcely studied by experimental methods.

It is well-known that the h^+ transfer mechanism on the TiO_2 surface should involve two processes: the photoinduced holes interact with surface active sites to form active paramagnetic intermediates, and then the active paramagnetic intermediates react with surface-adsorbed molecules. As such, besides the surface active sites, the active paramagnetic intermediates also play an important role in the photoreaction. Some paramagnetic intermediates (such as $^{\bullet}OH$, Ti−O^-, and O_2^-, etc.) have been experimentally observed. The $^{\bullet}OH$ radical was usually considered as the active paramagnetic intermediates which govern the photocatalytic oxidation reaction.[4,17,18] Nosaka and co-workers[7] pointed out that the photogenerated h^+ oxidation on the TiO_2 surface produced no free $^{\bullet}OH$ radicals but adsorbed $^{\bullet}OH$ (Ti$^{\bullet}$OH or TiO^-) radicals. However, it was also reported by measuring the quantum yield of $^{\bullet}OH$ radicals that their formation was not the major process on the TiO_2 surface in aqueous solutions under irradiation, while the $^{\bullet}OH$ radicals were produced from the oxidation of H_2O by O_2^-.[19] On the other hand, some previous studies[20,21] proposed that the O_2^- ion should be the active paramagnetic intermediate, which dictated the photodegradative oxidation reaction. Up to now, there have been no experimental studies on the detailed formation and transformation mechanism of various active paramagnetic intermediates in the photocatalytic H_2O splitting or H_2O oxidation, which may hinder the deep understanding of the surface photoinduced hole-transfer mechanism.

Solid-state NMR spectroscopy is a powerful tool for exploring the local environments of active sites in various photocatalysts.[22−25] Especially, the ^1H MAS NMR techniques have been widely used to study the structure and distribution of hydroxyl groups and adsorbed H_2O on the surface of TiO_2 and other oxides.[13−16] In addition, in situ solid-state NMR has been ultilized to study the photocatalytic reaction mechanism, focusing on the conversion of organic reagents on the photocatalyst surface.[26−28] However, little attention has been paid to the roles of both surface Ti−OH groups and absorbed H_2O in the photocatalytic reaction. Herein, TiO_2 photocatalysts with different Ti−OH groups and different loadings of adsorbed H_2O were studied by the solid-state NMR and electron spin resonance (ESR) techniques. One-dimensional (1D) ^1H solid-state magic angle spinning (MAS) NMR was employed to identify surface hydroxyl groups and adsorbed water molecules, while two-dimensional (2D) ^1H−^1H double-quantum (DQ) MAS NMR was utilized to provide the spatial proximity/interaction between them in the TiO_2 photocatalysts. Combining these NMR methods with in situ ^1H and ^{13}C NMR methods, besides the reaction intermediates, the surface active center and its quantitative structure−activity relationship were identified. Furthermore, the evolution of paramagnetic intermediates on the TiO_2 surface with varying H_2O loading upon irradiation was revealed for the first time by the in situ ESR technique. On the basis of the NMR and ESR results, the detailed photocatalytic mechanism of water splitting on the surface of TiO_2 was proposed.

2. EXPERIMENTAL SECTION

2.1. Sample Preparation. The Pt-loaded TiO_2 catalyst was prepared by in situ photodeposited reaction of H_2PtCl_6 with TiO_2 according to a previous report.[29] Briefly, 0.2 g of TiO_2 (Degussa P25, 41 m^2/g Brunauer−Emmett−Teller (BET) surface area, purchased from Sigma-Aldrich) was suspended in an aqueous solution containing H_2O (10 mL, deionized water) and $H_2PtCl_6{\cdot}6H_2O$ (0.618 mmol/L, purchased from Aladdin). After 2 h of irradiation under a 300 W Hg lamp, the gray product was collected via centrifugation, then washed by water, and dried at 333 K. The Pt/TiO_2 photocatalyst (denoted as PT-1) was obtained from the gray product by dehydrating it on a vacuum system (10^{-3} Pa) at 473 K for 10 h. The PT-1 photocatalyst was further dehydrated on the vacuum system (10^{-3} Pa) at 673 K for 10 h, and the obtained sample is denoted as PT-2.

Prior to ^1H MAS NMR measurements, the dehydrated photocatalysts (0.10 g) were directly transferred into 4 mm NMR rotors under a dry nitrogen atmosphere in a glovebox. To prepare the hydrated photocatalysts with different H_2O loadings, a certain amount of deionized H_2O was introduced into the dehydrated Pt/TiO_2 photocatalysts (PT-1 and PT-2) in a glass tube under vacuum at the temperature of liquid N_2, then the glass ampule was sealed off, and finally the sealed samples were transferred into the NMR rotors in the glovebox.

Prior to in situ NMR measurements, $^{13}CH_3OH$ (99% ^{13}C, 3.0 μmol, Cambridge Isotope Laboratories, Inc.) and deionized H_2O were introduced into the dehydrated Pt/TiO_2 catalyst (0.10 g) in a glass ampule under vacuum at the liquid N_2 temperature, and then the glass ampule was sealed off. The photoreaction was performed in the sealed ampule under successive irradiation by a 300 W Xe lamp, and then the ampule was transferred into a 7.5 mm rotor for in situ NMR measurements.

For ESR measurements, the dehydrated Pt/TiO_2 photocatalysts (0.10 g) were directly transferred into a 5 mm ESR quartz tube with a vacuum valve under a dry nitrogen atmosphere in a glovebox. Different amounts of H_2O molecules were also introduced into dehydrated Pt/TiO_2 photocatalysts in the ESR quartz tube under vacuum at the liquid N_2 temperature. The photoreaction was performed in the quartz tube under successive irradiation by a 300 W Xe lamp for a specific reaction period (30 min). After 30 min of solar-light irradiation, 0.5 μmol of CH_3OH was introduced into the hydrated photocatalysts in the ESR quartz tube under vacuum at the liquid N_2 temperature.

2.2. Characterization Methods. ^1H MAS NMR experiments were carried out at 11.7 T on a Bruker-Advance^{III} 500 spectrometer equipped with a 4 mm double-resonance probe. The resonance frequency was 500.57 MHz. Single-pulse excitation ^1H MAS experiments were performed on hydrated or dehydrated TiO_2 samples, by using a $\pi/2$ pulse width of 4.0 μs, a repetition time of 2 s, and a magic angle spinning rate of 10 kHz. Double-quantum coherences were excited and reconverted with the POST-C7 pulse sequence, and the excitation and reconversion time is equal to a complete C7 cycle (τ = 200 μs). The increment interval in the indirect dimension was set to 50 μs, and 32 t_1 increments and 1024 scan accumulations for each t_1 increment were used in the 2D ^1H−^1H DQ MAS NMR experiments. The spin−spin relaxation time (T_2) of different ^1H species was measured by the Hahn spin-echo technique. 2D ^1H−^1H NOESY correlation NMR spectra were acquired with mixing times of 10 and 80 ms, in which the increment interval in the indirect dimension was set to 83.3 μs, and 128 t_1 increments and 128 scan accumulations for each t_1 increment were used.

In situ ^1H and ^{13}C solid-state MAS NMR experiments were carried out at 7.1 T on a Varian Infinityplus-300 spectrometer, equipped with a double-resonance 7.5 mm probe, with resonance frequencies of 299.78 and 75.38 MHz for ^1H and ^{13}C, respectively. ^1H MAS experiments were carried out with a $\pi/2$ pulse width of 5.0 μs and a repetition time of 2 s. ^{13}C MAS experiments with ^1H decoupling were performed by using a $\pi/2$ pulse width of 5.5 μs and a repetition time of 2 s. The magic angle spinning rate was set to 3.5 kHz. The chemical shifts of ^1H and ^{13}C were referenced to adamantane (1.91 ppm for ^1H, 29.9 ppm for ^{13}C-methyl, and 39.0 ppm for ^{13}C-methylene).

ESR experiments were carried out at the X-band using a JEOL FA 2000 spectrometer. The microwave frequency was 9.1 GHz, the modulation amplitude was 0.1 mT, the microwave power was 5 mW, and the experimental temperature was 295 K. The g values of the radical species were referenced to a Mn marker.

DOI: 10.1021/jacs.7b04877
J. Am. Chem. Soc. 2017, 139, 10020−10028

3. RESULTS AND DISCUSSION

3.1. Surface Hydroxyl Groups and Adsorbed H_2O on Pt/TiO_2 Catalysts Studied by Solid-State ^1H MAS NMR.

To clarify the structure and distribution of Ti−OH groups and adsorbed H_2O on the surface of Pt/TiO_2 catalysts, 1D and 2D ^1H solid-state MAS NMR techniques were utilized. Figure 1a shows the 1D ^1H MAS spectrum of the Pt/TiO_2 catalyst (PT-1) dehydrated at 473 K. It can be seen that two types of surface hydroxyl groups are present, consistent with previous reports.[13−16,30] The signals at ca. 1.8 and 7.3 ppm can be assigned to terminal hydroxyl groups (OH_T) and bridging hydroxyl groups (OH_B), respectively,[13−16] while the small sharp signal at 0 ppm is due to the small amount of impurities (silicone grease, amounts to ca. 2.8% of the total proton content, Figure S1 in the Supporting Information). For the Pt/TiO_2 catalyst (PT-2) dehydrated at 673 K, the OH_T groups are predominant on the surface of TiO_2, while the OH_B groups are largely diminished (Figure 1b), indicating that the OH_B groups are preferentially removed by the high-temperature dehydration. By careful spectral deconvolution, we found that when additional H_2O is absorbed onto the PT-2 sample, the OH_B groups (7.3 ppm) are gradually recovered (Figure 1c,d), while the amount of OH_T groups remains almost constant with increasing H_2O loadings. The regeneration of OH_B groups may be attributed to the reaction of adsorbed H_2O molecules with oxygen vacancies which are usually produced on the TiO_2 surface during high-temperature vacuum treatment. When the H_2O loading increases to ca. 0.9 μmol on PT-2 (Figure 1d), the amount of OH_B groups is similar to that on PT-1 (Figure 1a). As such, the amount of surface OH_B groups should be approximately equal to the proton amount of adsorbed H_2O (ca. 1.8 μmol). With further increasing the H_2O loading to 1.1 μmol on PT-2, besides the two signals of Ti−OH groups (1.8 and 7.3 ppm), a signal at ca. 5.2 ppm due to surface-adsorbed H_2O appears, and it grows gradually with the increase of the H_2O loadings (Figure 1e−h). A similar trend is observable for PT-1 with the H_2O loading being increased from 0.2 to 2.7 μmol (Figure S2 in the Supporting Information).

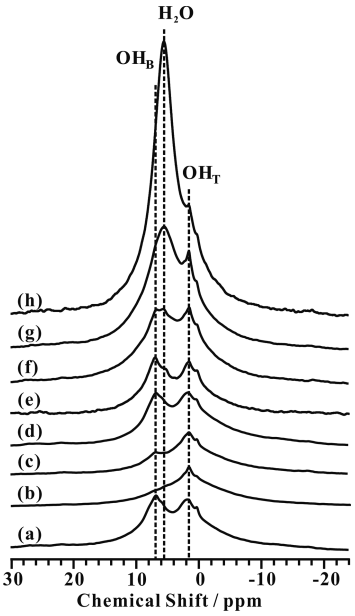

Figure 1. ^1H MAS NMR spectra of (a) bare PT-1 (Pt/TiO_2 dehydrated at 473 K), (b) bare PT-2 (Pt/TiO_2 dehydrated at 673 K), and (c−h) PT-2 loaded with different amounts of H_2O: (c) 0.5 μmol, (d) 0.9 μmol, (e) 1.1 μmol, (f) 2.0 μmol, (g) 2.7 μmol, and (h) 3.6 μmol.

2D $^1H-^1H$ DQ MAS NMR spectroscopy is a powerful method for probing proton−proton proximities/interactions in various solid materials[31−34] and was employed here to investigate the spatial proximities of various Ti−OH groups and the absorbed H_2O. The presence of a signal in the $^1H-^1H$ DQ MAS NMR spectrum indicates that two protons are in close proximity (<5 Å), as the DQ coherences observed are strongly dependent on the internuclear distance. Peaks that occur along the diagonal (ω, 2ω) are autocorrelation peaks resulting from the dipolar interaction of protons with the same chemical shift, while pairs of off-diagonal peaks at (ω_a, $\omega_a + \omega_b$) and (ω_b, $\omega_a + \omega_b$) correspond to correlations between two protons with different chemical shifts. As shown in Figure 2a, the 2D $^1H-^1H$ DQ MAS NMR spectrum of PT-2 shows only one diagonal peak at (1.8, 3.6) ppm due to the autocorrelation of OH_T groups, indicating that they are in close spatial proximity to each other. For PT-2 with a 0.9 μmol H_2O loading, two diagonal peaks at (1.8, 3.6) and (7.3, 14.6) ppm are observable (Figure 2b), corresponding to the autocorrelations of OH_T and OH_B groups, respectively. This suggests that the OH_T groups are only in close spatial proximity to other OH_T groups, and the OH_B groups are also only in close spatial proximity to other OH_B groups. The possible reason is that the two different types of Ti−OH groups may be present on different crystal planes of TiO_2. After 1.1 μmol of H_2O is introduced onto PT-2, four autocorrelation peaks can be identified in the $^1H-^1H$ DQ MAS spectrum (Figure 2c). Again, the autocorrelation peaks at (1.8, 3.6) and (7.3, 14.6) ppm correspond to the spatial proximity of OH_T and OH_B groups, respectively. The new autocorrelation peak at (5.2, 10.4) ppm can be ascribed to the spatial proximity of the hydrogen atom of adsorbed H_2O. Another new autocorrelation peak appears at (6.9, 13.8) ppm, and it grows with the consumption of the autocorrelation peak at (7.3, 14.6) ppm when the H_2O loading is gradually increased from 1.1 to 3.6 μmol (Figure 2c−f). As such, the signal at 6.9 ppm can be assigned to the ^1H signal of the OH_B group in hydrogen-bonding interaction with surface-adsorbed H_2O. Besides the autocorrelation peaks, an intense off-diagonal peak pair at (5.2, 12.1) and (6.9, 12.1) ppm is observable as well, corresponding to the spatial correlation between the surface-adsorbed H_2O and the bridging hydroxyl (OH_B) groups. It is interesting to note that even when the amount of adsorbed H_2O exceeds that of OH_B groups (1.8 μmol), the surface-adsorbed H_2O is only correlated to OH_B groups rather than OH_T groups (Figure 2e). All these findings indicate that surface H_2O only adsorbs on OH_B groups through hydrogen-bonding interaction, forming hydrated OH_B groups, which is crucial to the photocatalytic reaction (see below).

To study the dynamics of different ^1H species (OH_T, OH_B, and adsorbed H_2O) in the Pt/TiO_2 photocatalysts, we have measured their spin−spin relaxation time (T_2). Figure 3 shows the change of T_2 values for the different ^1H species in the PT-1 sample as a function of the H_2O loading. When the H_2O loading is low, the three ^1H species have similar T_2 values. With the increase of the H_2O loading, the T_2 values of both adsorbed H_2O and OH_B considerably decrease, while that of OH_T slightly declines. Generally, a smaller T_2 value should indicate a weaker mobility, and vice versa. Thus, the proton mobility of both adsorbed H_2O and OH_B is largely reduced with the

DOI: 10.1021/jacs.7b04877
J. Am. Chem. Soc. 2017, 139, 10020−10028

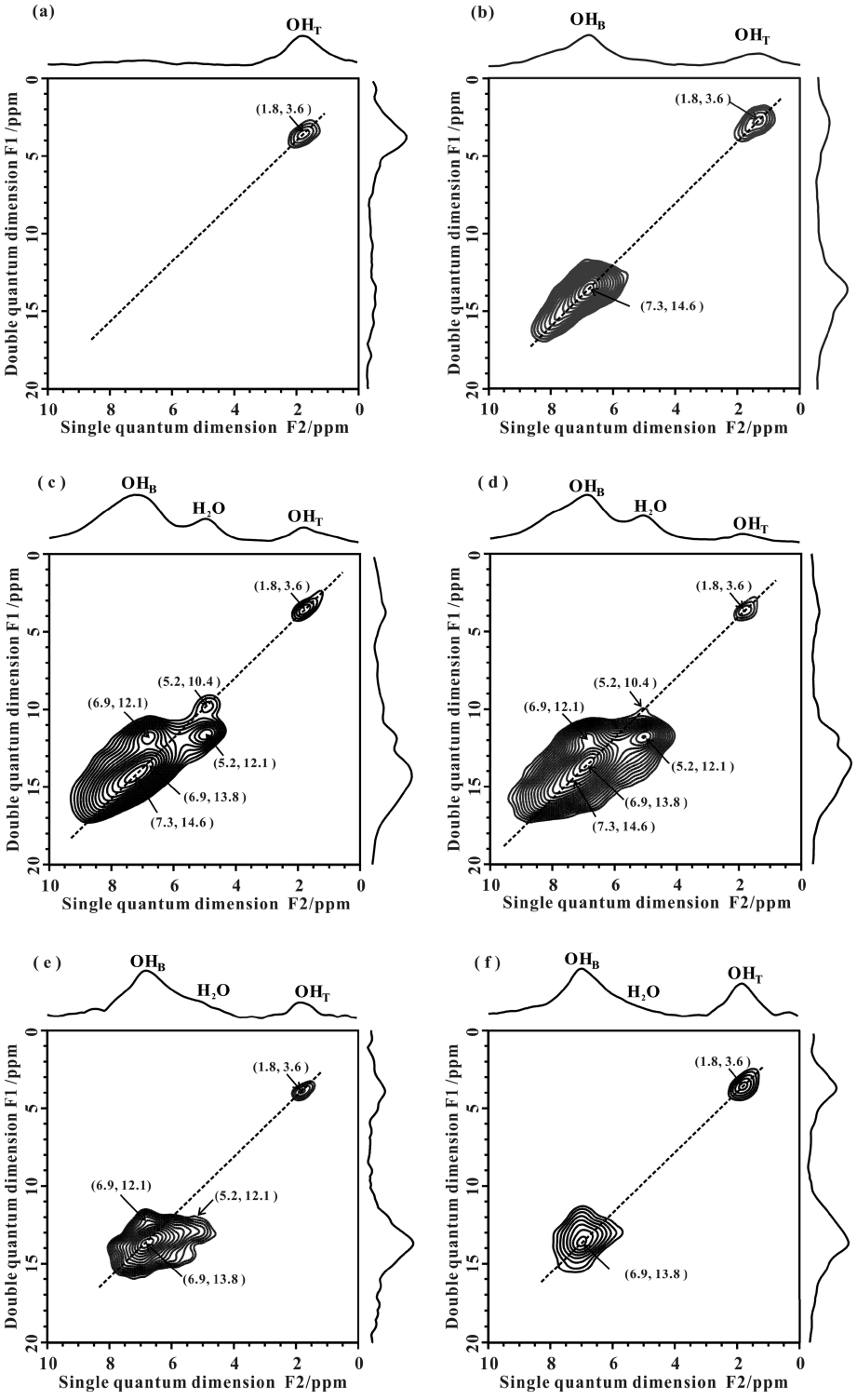

Figure 2. 2D ^{1}H−^{1}H DQ MAS NMR spectra of (a) bare PT-2 and (b−f) PT-2 loaded with different amounts of H_2O: (b) 0.9 μmol, (c) 1.1 μmol, (d) 2.0 μmol, (e) 2.7 μmol, and (f) 3.6 μmol.

increase of the H_2O loading as compared to OH_T, which could be ascribed to the interaction between adsorbed H_2O and OH_B. This result suggests that, with respect to OH_B, the OH_T should be present in a different chemical environment in which the interaction between OH_T and H_2O is very weak. A similar result can also be derived from the 2D ^{1}H−^{1}H NOESY correlation NMR spectra acquired with different mixing times for hydrated PT-1 (Figure S3 in the Supporting Information). As shown in Figure S3, at a short mixing time (10 ms), the correlation between OH_B and H_2O is observable, while the correlations between OH_T and OH_B/H_2O are absent, which is consistent with the ^{1}H−^{1}H DQ experimental result. At a long mixing time (80 ms), the correlations between OH_T and OH_B/H_2O appear, implying that only long-range/weak interactions are present between OH_T and OH_B/H_2O.

DOI: 10.1021/jacs.7b04877
J. Am. Chem. Soc. 2017, 139, 10020−10028

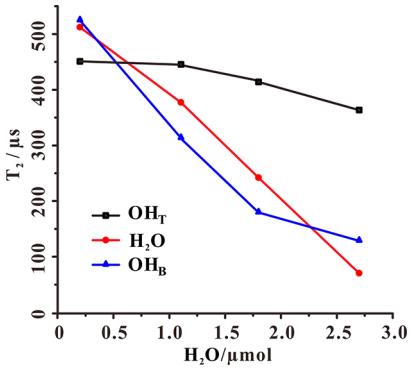

Figure 3. Spin–spin relaxation time (T_2) of different ^{1}H species (OH_T, OH_B, and adsorbed H_2O) in the PT-1 sample as a function of the H_2O loading.

3.2. Structure–Activity Relationship of Ti–OH and Adsorbed H_2O Studied by In Situ NMR Techniques. The photocatalytic hydrogen production processes from coadsorption of water and methanol on Pt/TiO_2 catalysts were characterized as functions of the irradiation time and H_2O loadings by in situ ^{13}C and ^{1}H solid-state MAS NMR techniques. Figure 4 shows the typical in situ ^{13}C and ^{1}H

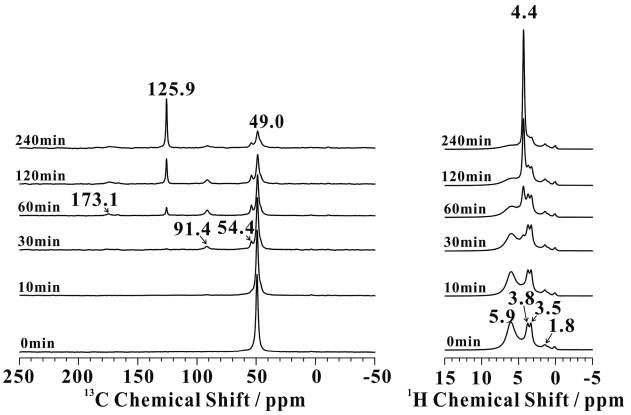

Figure 4. In situ ^{13}C (left) and ^{1}H (right) MAS NMR spectra of photocatalytic H_2 production from water splitting (methanol was used as a sacrifice reagent) as a function of solar-light irradiation over PT-1 loaded with 2.7 μmol of H_2O and 3.0 μmol of methanol.

MAS NMR spectra of PT-1 photocatalysts coadsorbed with 3.0 μmol of $^{13}CH_3OH$ and 2.7 μmol of H_2O as a function of the irradiation time ranging from 0 to 240 min. At 30 min of irradiation, in addition to the signal of unreacted $^{13}CH_3OH$ at 49.0 ppm,[35] two weak signals appear at 54.4 and 91.4 ppm, which can be assigned to dimethoxymethane (derived from the acetalization of HCHO and CH_3OH).[36] The oxidation of CH_3OH proceeds with the irraditation time being increased to 60 min, which is evidenced by the increase of dimethoxymethane and the appearance of carbon dioxide (δ = 125.9 ppm)[27] and formic acid (δ = 173.1 ppm).[37] Further prolonging the irradiation time from 60 to 240 min leads to an increase of carbon dioxide at the expense of methanol, dimethoxymethane, and formic acid. It can be deduced that methanol is successively photo-oxidized to form dimethoxymethane, formic acid, and carbon dioxide, which is consistent with the previous reports.[38,39] On the other hand, in situ ^{1}H MAS NMR spectra (Figure 4, right) were recorded to detect the H_2 production as a function of the irradiation time, in which the strong broad signal at 5.9 ppm can be assigned to the fast proton exchange among surface-hydrated OH_B, adsorbed H_2O, and the hydroxyl of CH_3OH, the signals at 3.8 and 3.5 ppm are due to the J-coupling peaks[40] of ^{1}H–^{13}C in the methyl group of CH_3OH, and the signal at 1.8 ppm is due to the surface OH_T group. When the irradiation time is increased to 30 min, the production of H_2 (δ = 4.4 ppm) is evident, and the amount of H_2 gradually increases with the consumption of the protons of H_2O, OH_B, and CH_3OH with further increasing the irradiation time.

The photocatalytic reaction processes on both PT-1 and PT-2 photocatalysts with different Ti–OH groups and variable H_2O loadings were thoroughly studied by in situ ^{13}C and ^{1}H NMR techniques (see Figures S4 and S5 in the Supporting Information). On the basis of the in situ NMR results, the evolution of the apparent rate constant of photocatalytic H_2 production (determined by calculating the integral area of the ^{1}H NMR signal of H_2 as a function of the solar-light irradiation time) as a function of the H_2O loading over PT-1 and PT-2 photocatalysts was ascertained (Figure 5a). It can be found that the photocatalytic activity of PT-1, on which both OH_B and OH_T groups are present, is negligible in the absence of adsorbed H_2O, implying that the presence of CH_3OH and Ti–OH on the surface of TiO_2 does not result in the transfer of the

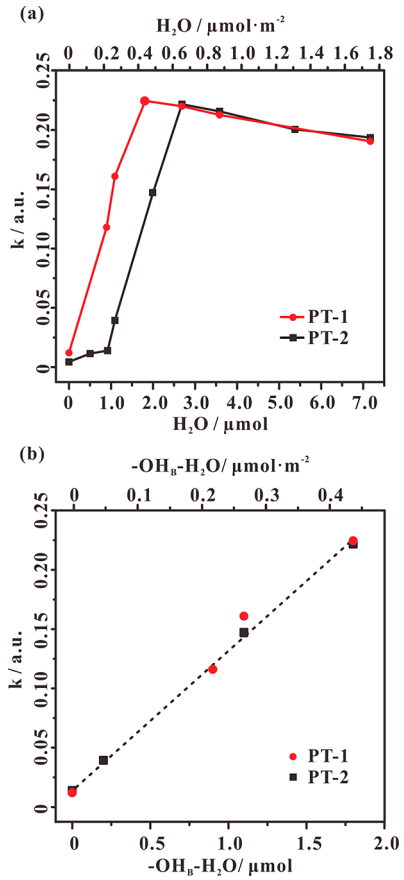

Figure 5. Evolution of the apparent rate constant of the photocatalytic water splitting reaction as functions of the water loading (a) and amount of hydrated OH_B groups (b) on PT-1 (red) and PT-2 (black) photocatalysts. The apparent rate constant was determined by calculating the integral area of the ^{1}H NMR signal of H_2 as a function of the solar-light irradiation time.

DOI: 10.1021/jacs.7b04877
J. Am. Chem. Soc. 2017, 139, 10020–10028

photoinduced hole to adsorbed molecules. The photocatalytic activity is dramatically enhanced when the amount of adsorbed H_2O is increased from 0 to 1.8 μmol. When the amount of adsorbed H_2O is ca. 1.8 μmol, which is equal to the amount of surface OH_B groups, the photocatalytic activity reaches a maximum, while it slightly declines with further increasing the H_2O loading. This indicates that the innermost adsorbed H_2O molecules (such as those adsorbed on the OH_B groups through hydrogen bonds) should be crucial to the photocatalytic reaction, and have a significant impact on the photocatalytic activity. Compared with PT-1, the PT-2 photocatalyst, which mainly retains OH_T groups, exhibits a different evolution trend for the apparent rate constant as a function of the H_2O loading. The photocatalytic activity of PT-2 is slightly improved with the increase of the H_2O loading in the range of 0−0.9 μmol. Obviously, an "induction period" for the formation of surface active centers is present, during which the OH_B groups (with the ^1H chemical shift at 7.3 ppm; see Figure 1b,c,d) are regenerated due to the reaction of adsorbed H_2O molecules with oxygen vacancies. With further increasing the H_2O loading, the evolution trend of the photocatalytic activity of PT-2 is similar to that of PT-1. Obviously, the existence of OH_B groups is an essential prerequisite to the photocatalytic reaction. In addition, as revealed by our ^1H MAS NMR results, the surface H_2O adsorbs solely on the OH_B groups through hydrogen bonds to form hydrated OH_B groups. Thus, the correlation between the amount of hydrated OH_B groups and the photocatalytic activity was also established and is shown in Figure 5b. It can be seen that the photocatalytic activity is almost linearly enhanced with the increase of the hydrated OH_B content, and it reaches a maximum when the amount of hydrated OH_B groups increases to 1.8 μmol. With further increasing the H_2O loading, the amount of hydrated OH_B remains constant, and the photocatalytic activity does not increase but slightly declines (Figure 5a). Therefore, we can conclude that the hydrated OH_B group is essential to the photocatalytic reaction and should be the photocatalytic active site.

3.3. Active Paramagnetic Intermediates Studied by In Situ ESR. To gain insight into the role of hydrated OH_B groups in the photoinduced hole-transfer process, in situ ESR experiments were performed before and after 30 min of solar-light irradiation on the PT-1 catalysts with different H_2O loadings, and the results are shown in Figure 6. For the bare PT-1 sample, only a weak signal with a g value of 1.9996 due to a small amount of oxygen defects is visible before solar-light irradiation (Figure 6a, black line). This signal remains almost unchanged upon 30 min of solar-light irradiation (Figure 6a, red line), which can be attributed to the rapid recombination of photoinduced holes and electrons. Interestingly, when a small amount of H_2O (ca. 0.2 μmol) is adsorbed onto PT-1, a broad ESR signal appears upon the irradiation (Figure 6b, red line), corresponding to a simulated ESR signal at $g_\perp$ = 2.020 and $g_\parallel$ = 1.999 (Figure 6g). This ESR signal can be assigned to the photoinduced surface $Ti-O^-$ centers, arising from trapped photoinduced holes at surface oxygen.[41,42] It can be deduced that the introduction of adsorbed H_2O facilitates the formation of the surface paramagnetic centers. According to our NMR results (Figure 2), the surface H_2O adsorbs solely on the OH_B groups of TiO_2, leading to the formation of hydrated OH_B groups. As such, the presence of a small amount of hydrated OH_B groups would trigger the trapping and transfer of the photoinduced hole to form the $Ti-O^-$ active paramagnetic intermediate on the surface of TiO_2.

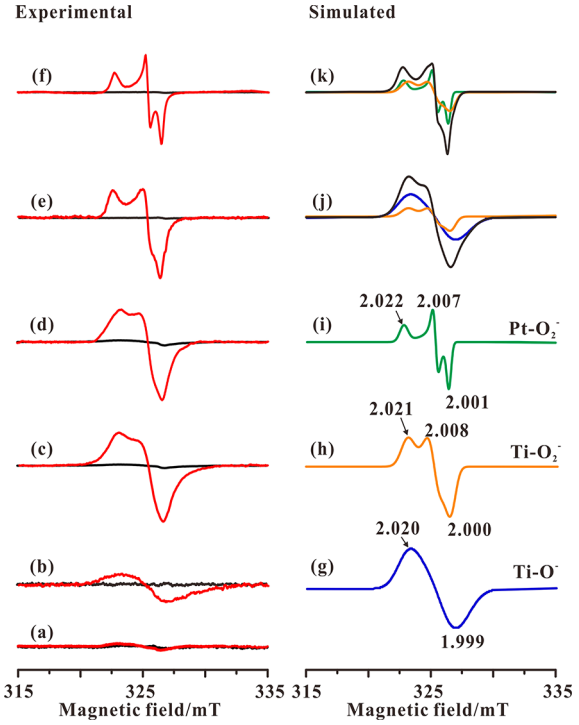

Figure 6. In situ ESR spectra (left) of PT-1 before (black line) and after (red line) 30 min of solar-light irradiation with different H_2O loadings: (a) 0 μmol, (b) 0.2 μmol, (c) 1.1 μmol, (d) 1.8 μmol, (e) 2.7 μmol, and (f) 3.6 μmol. Simulated spectra (right) of (g) $Ti-O^-$, (h) $Ti-O_2^-$, (i) $Pt-O_2^-$, (j) PT-1 loaded with 1.1 μmol of H_2O (the corresponding experimental spectrum is that in (c)), and (k) PT-1 loaded with 2.7 μmol of H_2O (the corresponding experimental spectrum is that in (e)).

When the H_2O loading is increased to 1.1 μmol (the amount of hydrated OH_B groups is 1.1 μmol), new ESR signals with g = 2.000−2.021 are visible upon solar-light irradiation (Figure 6c, red line), indicative of the formation of new surface paramagnetic species. According to previous reports,[43,44] the ESR signals of orthorhombic symmetry at g_{zz} = 2.021, g_{yy} = 2.008, and g_{xx} = 2.000 could be ascribed to surface superoxide $Ti-O_2^-$ sites. The O_2^- anion is usually stabilized on a metallic cationic site so that the electrostatic interaction splits the $2\pi^*$ antibonding orbitals by an amount (δ) due to the local cationic crystal field. The g_{zz} value can be measured by the equation $g_{zz} = g_e + 2\lambda/\delta$, where λ is the spin−orbit coupling constant of oxygen.[44] The g_{zz} value of 2.021 indicates that the O_2^- is stabilized at the Ti^{4+} cation.[44] To have a more detailed analysis, spectral simulations were performed. As shown in Figure 6j, the sum of the simulated spectra of surface $Ti-O^-$ (Figure 6g) and $Ti-O_2^-$ (Figure 6h) paramagnetic centers could well reproduce the experimental spectrum (Figure 6c) of PT-1 with a 1.1 μmol H_2O loading. Furthermore, to detect the stability of $Ti-O^-$ and $Ti-O_2^-$ centers, the evolution of ESR signals of the hydrated PT-1 sample as a function of the dark time was monitored by the in situ ESR technique (Figure 7a). By spectral simulation, we find that, with the increase of the dark time, the signal of $Ti-O^-$ gradually disappears, while only the orthorhombic signal of $Ti-O_2^-$ still exists even after 24 h.

When the H_2O loading is raised to 1.8 μmol, the content of hydrated OH_B groups reaches maximum (1.8 μmol). Only the

DOI: 10.1021/jacs.7b04877
J. Am. Chem. Soc. 2017, 139, 10020−10028

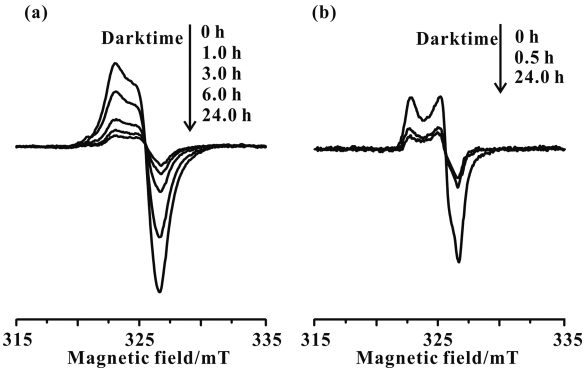

Figure 7. Evolution of ESR signals of PT-1 photocatalysts loaded with 1.1 μmol (a) and 2.7 μmol (b) of H_2O as a function of the dark time.

broad orthorhombic ESR signal (g_{zz} = 2.021, g_{yy} = 2.008, and g_{xx} = 2.000) of Ti−O_2^- is present and reaches a maximum, while the signal of Ti−O^- completely disappears upon solar-light irradiation (see parts d, red line, and h of Figure 6). Thus, with the increase of the hydrated OH_B content, the active paramagnetic intermediate is converted from Ti−O^- to Ti−O_2^- (the valence of the oxygen atom changes from −1 to −1/2). This indicates that increasing the trapping and transfer of photoinduced holes on the hydrated OH_B groups should be crucial for improving the activity of photocatalytic water splitting.

With further increasing the H_2O loading to 2.7 μmol, the amount of hydrated OH_B groups remains unchanged. In this case, the ESR signals (Figure 6e, red line) for active paramagnetic intermediates could be deconvoluted by two different components (Figure 6k): one corresponds to the residual Ti−O_2^- site, and the other with g_{zz} = 2.022, g_{yy} = 2.007, and g_{xx} = 2.001 (Figure 6i) is a typical ESR signal of weakly absorbed O_2^- species which is usually generated by the reduction of O_2 on metal-loaded zeolite catalysts.[45,46] Here we assign the signals with g_{zz} = 2.022, g_{yy} = 2.007, and g_{xx} = 2.001 to the weakly absorbed superoxide (Pt−O_2^-) arising from the reduction of O_2 by photoinduced electrons on the cocatalyst Pt. Therefore, when the amount of adsorbed H_2O exceeds that of saturation adsorption on the OH_B groups, the Ti−O_2^- center will be further oxidized to generate O_2 by the photoinduced hole. Part of the O_2 molecules interact with the cocatalyst Pt and then are reduced to form the weakly absorbed O_2^- species by photoinduced electrons, which should be responsible for the decrease of the ESR signal of active paramagnetic intermediates. Of course, the formed O_2 molecules can readily trap the photoinduced electron to regenerate Ti−O_2^- species as well on the surface of TiO_2 as previously reported.[47] The evolution of the ESR signals of the hydrated PT-1 photocatalyst as a function of the dark time was also studied by the in situ ESR technique. As shown in Figure 7b, only the orthorhombic signal of Ti−O_2^- is detectable after 24 h.

When the H_2O loading is increased to 3.6 μmol, only the narrow orthorhombic ESR signals of weakly adsorbed O_2^- species (g_{zz} = 2.022, g_{yy} = 2.007, and g_{xx} = 2.001) are observable upon solar-light irradiation (parts f, red line, and i of Figure 6). Although part of the O_2 molecules are consumed to trap the photoinduced electrons on the cocatalyst Pt, forming the Pt−O_2^- intermediate, the total amount of active paramagnetic intermediates decreased obviously, which should be responsible for the declined activity of photocatalytic water splitting. To validate the activity of these paramagnetic intermediates (Ti−O^-, Ti−O_2^-, and Pt−O_2^-), a small amount of methanol (ca. 0.5 μmol) was introduced onto the various hydrated PT-1 samples. It could be found that their ESR signals disappear completely upon solar-light irradiation (Figure S6 in the Supporting Information), and simultaneous oxidation of methanol occurs, indicating that all these paramagnetic intermediates possess high oxidation activity. Therefore, all these experimental results confirm that the hydrated OH_B group is the transfer channel of the photoinduced hole,

Scheme 1. Proposed Hole-Transfer Mechanism for Photocatalytic Water Splitting on the TiO_2 Photocatalyst upon Solar-Light Irradiation

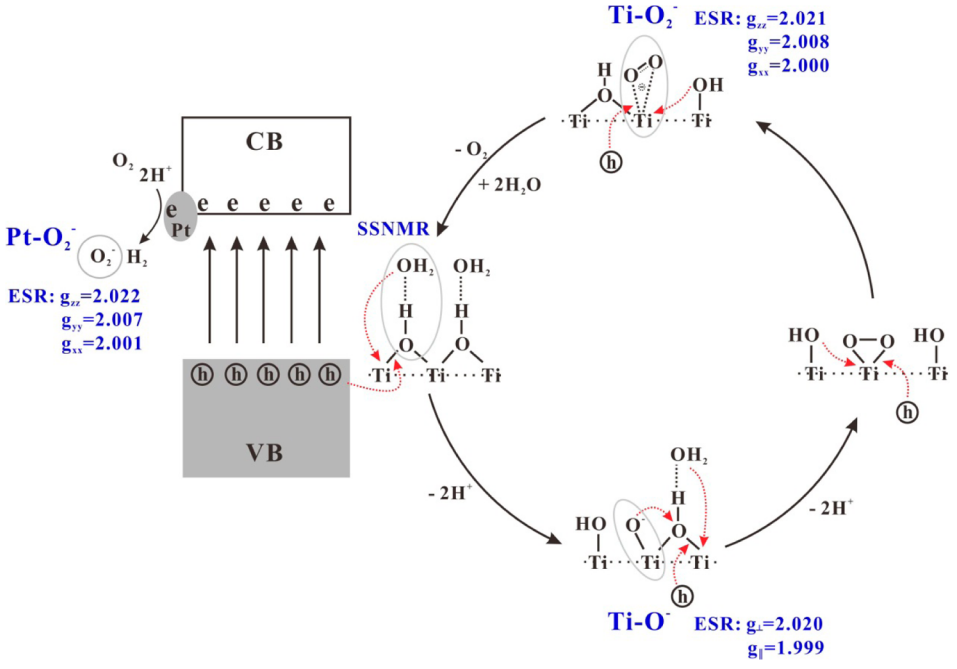

DOI: 10.1021/jacs.7b04877
J. Am. Chem. Soc. 2017, 139, 10020−10028

which controls the oxidation of both adsorbed H_2O and organic compounds on the TiO_2 surface.

3.4. Photocatalytic Mechanism. Hydrogen production (reduction of H^+ by photoinduced electron) proceeds on the Pt cocatalyst in this case, while the oxidation of the photoinduced hole is characterized by the formation of active radicals on the surface active sites of TiO_2 for oxidation of water and organic compounds. The above NMR and ESR experimental results allow us to propose the hole-transfer mechanism for photocatalytic water splitting on the TiO_2 photocatalyst upon solar-light irradiation, as illustrated in Scheme 1. According to our NMR and ESR experimental results, it can be concluded that the hydrated OH_B groups are the photocatalytic active sites to trap the photoinduced holes, which trigger the oxidation of water and organic compound. Theoretical results[11,12] also suggested that the mismatch between the valence band of TiO_2 and the O 2p levels of Ti−OH groups and adsorbed H_2O could be overcome by the overpotential created by the photoinduced hole in the vicinity of Ti−OH groups. As shown in Scheme 1, upon solar-light irradiation, the hydrated OH_B groups trap a photoinduced hole to generate the $Ti-O^-$ intermediate associated with the ESR signal at $g_\perp = 2.020$ and $g_\parallel = 1.999$. Meanwhile, a nucleophilic attack of adsorbed H_2O to the hole-trapped sites occurs, which hinders the recombination of photoinduced electrons and holes (i.e., the recombination of $Ti-O^-$ with the adjacent Ti sites), and thereby stabilizes the formation of $Ti-O^-$ species. It is noteworthy that when the amount of adsorbed H_2O is low on the TiO_2 surface, only an isolated hydrated OH_B group is present, and thus, only the $Ti-O^-$ species is formed and stabilized under solar-light irradiation. With the increase of the amount of adsorbed H_2O, the hydrated OH_B groups increase gradually and are adjacent to each other. When another photoinduced hole is trapped by a neighboring hydrated OH_B group and the hole-trapped site is nucleophilicly attacked by another adsorbed H_2O, two adjacent $Ti-O^-$ centers can couple with each other to form surface peroxide species as shown in Scheme 1. It was previously reported that the H_2O_2 could react with TiO_2 powder, forming surface O_2^- anions.[48] As such, the surface peroxide intermediate would be oxidized by the photoinduced hole to form $Ti-O_2^-$ species associated with the ESR signals with $g_{zz} = 2.021$, $g_{yy} = 2.008$, and $g_{xx} = 2.000$. Meanwhile, the nucleophilic attack of an adjacent OH_T group on the Ti atom leads to the recovery of OH_B group, which favors the formation and stabilization of the $Ti-O_2^-$ center. A further oxidation of the $Ti-O_2^-$ center by the photoinduced hole results in the formation of an O_2 molecule followed by the recovery of another OH_B group arising from the nucleophilic attack of an adjacent OH_T. The excessive H_2O molecules adsorb on the regenerated OH_B groups, which may hinder the interaction between the O_2 molecule and the TiO_2 surface, and further prevent the O_2 molecule from trapping the photoinduced electron to form $Ti-O_2^-$ species. Then the O_2 molecule would interact with the cocatalyst Pt and be reduced to form $Pt-O_2^-$ species by the photoinduced electron. This is consistent with our experimental observation that when the amount of adsorbed H_2O exceeds the saturation adsorption capacity of OH_B groups, the ESR signal of $Pt-O_2^-$ begins to appear as shown in Figure 6e,f. Actually, the $Pt-O_2^-$ species were usually assumed to be the active radicals for oxidation of organic compounds in actual photocatalytic reactions of the TiO_2 system with massive H_2O molecules.[49,50] As such, the O_2^- species can be consumed by the sacrificial reagent (methanol) to hinder the consumption of photoinduced electrons, while the reduction of O_2^- species by the photoinduced electron ($O_2^- + 2H^+ + e \rightarrow H_2O_2 + 2H^+ + 2e \rightarrow 2H_2O$) should be responsible for the low efficiency of the photocatalytic pure water splitting. On the other hand, the reduction of H^+ arising from OH_B groups and adsorbed H_2O by photoinduced electrons on the cocatalyst Pt produces the H_2 molecule.

4. CONCLUSIONS

In summary, the surface active sites and the photocatalytic mechanism of water splitting on the surface of Pt/TiO_2 catalysts have been investigated by solid-state NMR and in situ ESR techniques. Our experimental results unambiguously demonstrated that the hydrated OH_B groups were the surface active sites during photocatalytic water splitting, and the quantitative correlation between the amount of hydrated OH_B groups and the photoactivity of water splitting was established for the first time. The evolution of paramagnetic active intermediates on the TiO_2 surface with different amounts of surface-adsorbed H_2O under solar-light irradiation was monitored by in situ ESR spectroscopy, which revealed that the hydrated OH_B groups offer a channel for the transfer of the photogenerated hole in the photocatalytic reaction. On the basis of the experimental observations, we proposed the detailed hole-transfer mechanism for photocatalytic water splitting on the TiO_2 photocatalyst. The results presented herein should not only facilitate a better understanding of the photocatalytic mechanism at the atomic level but also be helpful for the rational design of highly active titania-based photocatalysts.

■ ASSOCIATED CONTENT

Supporting Information

The Supporting Information is available free of charge on the ACS Publications website at DOI: 10.1021/jacs.7b04877.

Spectral deconvolution of the ^1H MAS NMR spectrum of PT-1, ^1H MAS spectra of PT-1 with various H_2O loadings, 2D $^1H-^1H$ NOESY correlation NMR spectra of hydrated PT-1 acquired with different mixing times, in situ ^{13}C and ^1H MAS NMR spectra of the photocatalytic reaction on PT-1 and PT-2 photocatalysts with different Ti−OH groups and variable H_2O loadings, and in situ ESR spectra before and after 0.5 μmol of methanol being introduced to PT-1 with different H_2O loadings (PDF)

■ AUTHOR INFORMATION

Corresponding Authors

*ningdong.feng@wipm.ac.cn
*dengf@wipm.ac.cn

ORCID

Jun Xu: 0000-0003-2741-381X
Feng Deng: 0000-0002-6461-7152

Notes

The authors declare no competing financial interest.

■ ACKNOWLEDGMENTS

This work was supported by the National Natural Science Foundation of China (Grant Nos. 21673283, 21473246, and 21210005).

DOI: 10.1021/jacs.7b04877
J. Am. Chem. Soc. 2017, 139, 10020−10028

REFERENCES

(1) Nakamura, R.; Nakato, Y. *J. Am. Chem. Soc.* **2004**, *126*, 1290.
(2) Tamaki, Y.; Furube, A.; Murai, M.; Hara, K.; Katoh, R.; Tachiya, M. *J. Am. Chem. Soc.* **2006**, *128*, 416.
(3) Imanishi, A.; Okamura, T.; Ohashi, N.; Nakamura, R.; Nakato, Y. *J. Am. Chem. Soc.* **2007**, *129*, 11569.
(4) Jaeger, C. D.; Bard, A. J. *J. Phys. Chem.* **1979**, *83*, 3146.
(5) Takahashi, K.; Yui, H. *J. Phys. Chem. C* **2009**, *113*, 20322.
(6) Tan, S.; Feng, H.; Ji, Y.; Wang, Y.; Zhao, J.; Zhao, A.; Wang, B.; Luo, Y.; Yang, J.; Hou, J. G. *J. Am. Chem. Soc.* **2012**, *134*, 9978.
(7) Nosaka, Y.; Komori, S.; Yawata, K.; Hirakawa, T.; Nosaka, A. Y. *Phys. Chem. Chem. Phys.* **2003**, *5*, 4731.
(8) Micic, O. I.; Zhang, Y. N.; Cromack, K. R.; Trifunac, A. D.; Thurnauer, M. C. *J. Phys. Chem.* **1993**, *97*, 7277.
(9) Salvador, P. *J. Phys. Chem. C* **2007**, *111*, 17038.
(10) Kisumi, T.; Tsujiko, A.; Murakoshi, K.; Nakato, Y. *J. Electroanal. Chem.* **2003**, *545*, 99.
(11) Valdes, A.; Qu, Z. W.; Kroes, G. J.; Rossmeisl, J.; Norskov, J. K. *J. Phys. Chem. C* **2008**, *112*, 9872.
(12) Valdes, A.; Kroes, G. J. *J. Phys. Chem. C* **2010**, *114*, 1701.
(13) Mastikhin, V. M.; Mudrakovsky, I. L.; Nosov, A. V. *Prog. Nucl. Magn. Reson. Spectrosc.* **1991**, *23*, 259.
(14) Soria, J.; Sanz, J.; Sobrados, I.; Coronado, J. M.; Maira, A. J.; Hernández-Alonso, M. D.; Fresno, F. *J. Phys. Chem. C* **2007**, *111*, 10590.
(15) Chary, K. V. R.; Vijayakumar, V.; Rao, P. K.; Nosov, A. V.; Mastikhin, V. M. *J. Mol. Catal. A: Chem.* **1995**, *96*, L5.
(16) Crocker, M.; Herold, R. H. M.; Wilson, A. E.; Mackay, M.; Emeis, C. A.; Hoogendoorn, A. M. *J. Chem. Soc., Faraday Trans.* **1996**, *92*, 2791.
(17) Anpo, M.; Shima, T.; Kubokawa, Y. *Chem. Lett.* **1985**, *14*, 1799.
(18) Liu, G.; Yang, H. G.; Wang, X.; Cheng, L.; Pan, J.; Lu, G. Q.; Cheng, H.-M. *J. Am. Chem. Soc.* **2009**, *131*, 12868.
(19) Ishibashi, K.; Fujishima, A.; Watanabe, T.; Hashimoto, K. *J. Photochem. Photobiol., A* **2000**, *134*, 139.
(20) Guan, H. L.; Lin, J.; Qiao, B. T.; Yang, X. F.; Li, L.; Miao, S.; Liu, J. Y.; Wang, A. G.; Wang, X. D.; Zhang, T. *Angew. Chem., Int. Ed.* **2016**, *55*, 2820.
(21) Wu, N. Q.; Wang, J.; Tafen, D.; Wang, H.; Zheng, J. G.; Lewis, J. P.; Liu, X. G.; Leonard, S. S.; Manivannan, A. *J. Am. Chem. Soc.* **2010**, *132*, 6679.
(22) Reyes-Garcia, E. A.; Sun, Y. P.; Reyes-Gil, K.; Raftery, D. *J. Phys. Chem. C* **2007**, *111*, 2738.
(23) Feng, N.; Zheng, A.; Wang, Q.; Ren, P.; Gao, X.; Liu, S.-B.; Shen, Z.; Chen, T.; Deng, F. *J. Phys. Chem. C* **2011**, *115*, 2709.
(24) Feng, N.; Wang, Q.; Zheng, A.; Zhang, Z.; Fan, J.; Liu, S.-B.; Amoureux, J.-P.; Deng, F. *J. Am. Chem. Soc.* **2013**, *135*, 1607.
(25) Feng, N.; Liu, F.; Huang, M.; Zheng, A.; Wang, Q.; Chen, T.; Cao, G.; Xu, J.; Fan, J.; Deng, F. *Sci. Rep.* **2016**, *6*, 34765.
(26) Hwang, S. J.; Petucci, C.; Raftery, D. *J. Am. Chem. Soc.* **1998**, *120*, 4388.
(27) Pilkenton, S.; Hwang, S. J.; Raftery, D. *J. Phys. Chem. B* **1999**, *103*, 11152.
(28) Wang, X. L.; Liu, W. Q.; Yu, Y. Y.; Song, Y. H.; Fang, W. Q.; Wei, D. X.; Gong, X. Q.; Yao, Y. F.; Yang, H. G. *Nat. Commun.* **2016**, *7*, 11918.
(29) Zong, X.; Yan, H. J.; Wu, G. P.; Ma, G. J.; Wen, F. Y.; Wang, L.; Li, C. *J. Am. Chem. Soc.* **2008**, *130*, 7176.
(30) Schaub, R.; Thostrup, P.; Lopez, N.; Laegsgaard, E.; Stensgaard, I.; Norskov, J. K.; Besenbacher, F. *Phys. Rev. Lett.* **2001**, *87*, 266104.
(31) Brown, S. P.; Spiess, H. W. *Chem. Rev.* **2001**, *101*, 4125.
(32) Trébosc, J.; Wiench, J. W.; Huh, S.; Lin, V. S. -Y.; Pruski, M. *J. Am. Chem. Soc.* **2005**, *127*, 3057.
(33) Li, S. H.; Zheng, A. M.; Su, Y. C.; Zhang, H. L.; Chen, L.; Yang, J.; Ye, C. H.; Deng, F. *J. Am. Chem. Soc.* **2007**, *129*, 11161.
(34) Bendjeriou-Sedjerari, A.; Pelletier, J. D. A.; Abou-hamad, E.; Emsley, L.; Basset, J.-M. *Chem. Commun.* **2012**, *48*, 3067.
(35) Zhang, H. L.; Zheng, A. M.; Yu, H. G.; Li, S. H.; Lu, X.; Deng, F. *J. Phys. Chem. C* **2008**, *112*, 15765.
(36) Liu, Y.; Zhao, S.-F.; Guo, S.-X.; Bond, A. M.; Zhang, J.; Zhu, G.; Hill, C. L.; Geletii, Y. V. *J. Am. Chem. Soc.* **2016**, *138*, 2617.
(37) Duncan, T. M.; Vaughan, R. W. *J. Catal.* **1981**, *67*, 49.
(38) Chen, T.; Feng, Z. H.; Wu, G. P.; Shi, J. Y.; Ma, G. J.; Ying, P. L.; Li, C. *J. Phys. Chem. C* **2007**, *111*, 8005.
(39) Kawai, T.; Sakata, T. *J. Chem. Soc., Chem. Commun.* **1980**, 694.
(40) Rutar, V. *J. Magn. Reson.* **1984**, *58*, 306.
(41) Howe, R. F.; Gratzel, M. *J. Phys. Chem.* **1987**, *91*, 3906.
(42) D'Arienzo, M.; Carbajo, J.; Bahamonde, A.; Crippa, M.; Polizzi, S.; Scotti, R.; Wahba, L.; Morazzoni, F. *J. Am. Chem. Soc.* **2011**, *133*, 17652.
(43) Attwood, A. L.; Murphy, D. M.; Edwards, J. L.; Egerton, T. A.; Harrison, R. W. *Res. Chem. Intermed.* **2003**, *29*, 449.
(44) Che, M.; Tench, A. J. *Adv. Catal.* **1983**, *32*, 1.
(45) Qi, G. D.; Xu, J.; Su, J. H.; Chen, J. F.; Wang, X. M.; Deng, F. *J. Am. Chem. Soc.* **2013**, *135*, 6762.
(46) Lee, C. W.; Saintpierre, T.; Azuma, N.; Kevan, L. *J. Phys. Chem.* **1993**, *97*, 11811.
(47) Berger, T.; Sterrer, M.; Diwald, O.; Knozinger, E. *ChemPhysChem* **2005**, *6*, 2104.
(48) Tengvall, P.; Lundstrom, I.; Sjoqvist, L.; Elwing, H.; Bjursten, L. M. *Biomaterials* **1989**, *10*, 166.
(49) Li, Y.; Wen, B.; Yu, C.; Chen, C.; Ji, H.; Ma, W.; Zhao, J. *Chem. - Eur. J.* **2012**, *18*, 2030.
(50) Chen, Q. H.; Liu, H. L.; Xin, Y. J.; Cheng, X. W.; Li, J. J. *Appl. Surf. Sci.* **2013**, *264*, 476.

DOI: 10.1021/jacs.7b04877
J. Am. Chem. Soc. 2017, 139, 10020−10028